Soft Matter

Accepted Manuscript

ROYAL SOCIETY OF CHEMISTRY

www.rsc.org/softmatter

Cite this: DOI: 10.1039/c0xx00000x

www.rsc.org/xxxxxx

ARTICLE TYPE

On the Two-step Phase Transition Behavior of the Poly(*N*-isopropylacryamide) (PNIPAM) Brush: Different Zones with Different Orders

Hui Tang, Bo Zhang and Peiyi Wu*

Received (in XXX, XXX) Xth XXXXXXXXX 20XX, Accepted Xth XXXXXXXXX 20XX
DOI: 10.1039/b000000x

Poly(*N*-isopropylacryamide) (PNIPAM) brushes integrating poly[oligo(ethylene glycol) methacrylate] (POEGMA) as the core, were prepared *via* successive atom transfer radical polymerization (ATRP). Dynamic thermal phase transition behavior of PNIPAM brushes was studied by means of IR spectroscopy in combination with the perturbation correlation moving window (PCMW) technique and two-dimensional correlation spectroscopy (2Dcos) analysis. Compared with aqueous dispersions of PNIPAM brushes covalently bound to the surface of gold nanoparticles and hydrophobic hyperbranched polyester core, increment of the double phase transition temperature was observed due to the existence of POEGMA core which was favourable to the hydrophilic condition. With PCMW analysis, the phase transition temperature (ca. 36 °C) as well as the transition temperature range (33–41 °C) during the heating process was determined. 2Dcos was employed to discern the sequence order of group motions during heating. It is concluded that the PNIPAM in the inner zone responses earlier than that located in the outer zone.

Introduction

Polymer brushes, ultrathin assemblies of polymer chains that are tethered to solid substrate or interface with sufficiently high density, have been widely studied in different application domains ranged from electronics to biology.[1-3] Especially, owing to the change in the conformation of grafted chains in response to external stimuli, polymer brushes comprising stimuli-responsive polymers have attracted enormous scientific attention with the aim to construct functionalized smart surfaces.[4,5] Considering the sharp and reversible phase transition of poly(*N*-isopropylacrylamide) (PNIPAM) at lower critical solution temperature (LCST) of ~32°C in water,[6-8] coil-to-globule type transitions have been measured by dynamic light scattering for PNIPAM chains attached to the surfaces of polystyrene latex particles dispersed in water.[9] Due to the steric exclusion between neighboring chains in the polymer brush, PNIPAM chains close to the core were densely packed with less hydrated, resulted in the lower transition temperature and wider temperature range compared with free PNIPAM chains in aqueous solutions.

Particularly, double phase transition of dilute aqueous dispersions of PNIPAM brushes covalently bound to the surface of gold nanoparticles (denoted as Au-PNIPAM) has been investigated by Tenhu *et al*.[10-12] Considering that the PNIPAM segments close to the core may be more densely packed compared with that close to the shell, a model with an inner less hydrated layer close to the hydrophobic core which account for the lower temperature transition and an outer more hydrated layer responsible for the higher one was explained. Similar results have also been reported in phase transition of unimolecular micelles with PNIPAM grafted on hydrophobic polyester core.[13,14] Since the concentration of PNIPAM segments in the inner part is higher than that in the outer part with polymer chains densely packed around the hydrophobic core, lower transition temperature can be explained by the interchain interactions in the zone close to the interface.[14-16] However, to the best of our knowledge, the effect of hydrophilicity of the core on the double phase transition behavior had seldom been discussed although it has been reported that the thermal phase behavior of PNIPAM may be manipulated by copolymerization with hydrophilic or hydrophobic monomers.[17,18]

Herein, polymer brush integrating PNIPAM and hydrophilic poly[oligo(ethylene glycol) methacrylate] (POEGMA) was synthesized *via grafting from* method.[19,20] Different from conventional brush copolymers in which high density bulky side chains are packed around the backbone and somewhat stretched, the long flexible ethylene glycol spacers decoupled the interaction between main chains and side chains and the large molar ratio between PNIPAM and POEGMA induced the copolymers to form core-shell morphology with coiled hydrophilic POEMGA main chains. The integrated dynamic mechanism was carefully studied by FT-IR spectroscopy in combination with two-dimensional correlation spectroscopy (2Dcos) and perturbation correlation moving window (PCMW) technique. The impacts of hydrophilic core and the structure on the phase behavior of copolymers were discussed and different zones with different orders during the phase transition process was analysed.

Experimental

Materials

Polymer brushes integrating PNIPAM side chains and hydrophilic POEGMA main chains (POEGMA-*g*-PNIPAM) were synthesized with *grafting from* method. Detailed synthesis procedure and characterization were described in the supporting information.

Methods

Perturbation correlation moving window (PCMW). Temperature-dependent FT-IR spectra collected with an increment of 1 °C were used to perform PCMW analysis. Primary data processing was carried out with the method provided by Morita and further correlation calculation was conducted using the software of 2D Shige ver. 1.3 (Shigeaki Morita, Kwansei Gakuin University, Japan, 2004-2005). The contour maps were plotted by Origin Program ver. 8.0 with red colors defined as positive intensities and blue colors as negative ones. An appropriate window size (2m+1=11) was chosen to generate PCMW spectra with good quality.

Two-dimensional correlation analysis (2Dcos). Temperature-dependent FT-IR spectra recorded at an internal of 1°C in certain wavenumber ranges were selected to perform 2D correlation analysis. 2D correlation analysis was conducted using 2D Shige ver. 1.3 (Shigeaki Morita, Kwansei Gakuin University, Japan, 2004-2005) and was further plotted into the contour maps by Origin Program ver. 8.0. In the contour maps, red colors are defined as positive intensities, while blue colors are defined as negative ones.

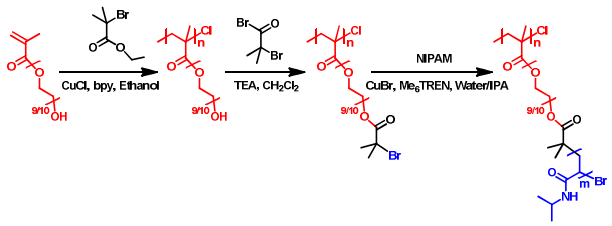

Scheme 1. Synthesis of POEMGA-*g*-PNIPAM

Results and discussion

Due to the decoupling effect of long flexible ethylene glycol spacers and the large molar ratio between PNIPAM and POEGMA, core-shell morphology with coiled POEMGA main chains may be observed in the copolymers. Notably, the aqueous solution display light blue at room temperature and the hydrodynamic radius of copolymer in water below LCST was around 100 nm, which is another evidence for the self-assembly nature and aggregate morphology (Fig S1). In the previous study of PNIPAM with hyperbranched poly(glycidol) as the core, spherical nanoparticles with diameter of 80nm were observed. A closer examination of the SEM image reveals that some unimolecular micelles seem to be in contact with each other, possible because of the concentration and drying effects during sample preparation for SEM.[21,22] In the present study, the hydrodynamic radius distribution may be in agreement with the dynamic LLS results of HPG–PNIPAM if molecular weight and solvation effects are taken into account.

Temperature-dependent ^{1}H NMR spectra of G100 in D_2O (10 wt %) from 25 to 45 °C with the increment of 2 °C was performed for analysis, as shown in Fig. 1. Normalization was performed according to the integrated intensity of HDO peak from the solvent. All the peaks corresponding to PNIPAM shift toward lower field along with drastic intensity decrease in the heating process.[23,24] Phase separation fraction p was employed to characterize the degree of phase transition, while p is defined as:

$$p = 1 - (I/I_0)$$

where I and I_0 are the normalized integrated intensities of a selected resonant peak at a specified temperature and 25 °C, respectively.[25,26] Temperature dependences of the phase separation fraction p for different proton types of G100 in D_2O are presented in Fig. 1b. The protons at the main chain of the segments of PNIPAM response earlier than that of the side chain of the segments of PNIPAM, which might be due to the higher density in the inner zone. Taking the middle point of the curves as the phase transition temperature (T_p), the T_p was determined to be *ca.* 34°C, which is in good accordance with that recognized from DLS and turbidity test (Fig S2). Additionally, a "sol-gel" transition when heated above LCST was observed in G100 aqueous solution with the concentration of more than 5% (Fig S3). Considering that PNIPAM aggregates were covalently connected by POEGMA and three-dimensional gel network was formed, the gel phenomenon was explained by the classical physical cross-linking mechanism.

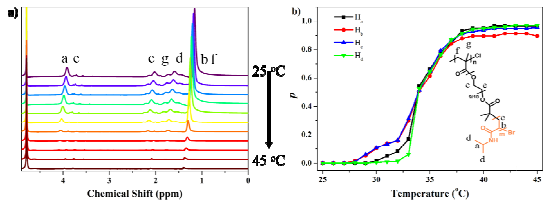

Fig. 1 (a) Normalized temperature-variable ^{1}H NMR spectra of G100 in D_2O (10 wt %); (b) Temperature dependences of phase separated fraction p for different protons.

Normalized temperature-variable ^{1}H NMR spectra of G25 and polymer blend composed of POEGMA and PNIPAM with the same proportion was also performed, as shown in Fig. 2. Since most part of POEGMA chain exist independently in the solution, the peak e corresponding to OEGMA side chain changed slightly in the blend system. The steady intensity of peak e also implied that the OEGMA segments have no temperature response in this temperature range. However, obvious intensity decrease was observed in G25 with temperature increment. It was inferred that the POEMGA was wrapped by PNIPAM and acted as the hydrophilic core in the phase transition process.

DSC curves of 10 wt% solution of copolymers was investigated (Fig. S4) and double endothermic peaks located at ~34 °C and ~36 °C were identified. Apparently, the lower temperature endothermic peak is relatively sharp compared with the higher temperature one. Notably, increment of the double phase transition temperature compared with that of the homopolymer was observed. The phenomenon of water stored close to the core has been discussed in Au-PNIPAM dispersions. Due to the restrictions on the collapse of the PNIPAM chain, water might remain finely dispersed within the polymer matrix and faster response of the dispersions compared to pure PNIPAM

has been observed.[12] In the present study, the hydrophilic domains within the vitrified polymer may hinder the transport of water molecules from the inner zone to the outer zone although hydrophilic channel which facilitated the diffusion of water molecules throughout the polymer matrix has been explained in PNIPAM with PEO grafts.[27] Therefore, higher phase transition temperature was observed. Additionally, due to the hydrophilic condition of POEGMA core, temperature difference of the double endothermic peaks decreased.

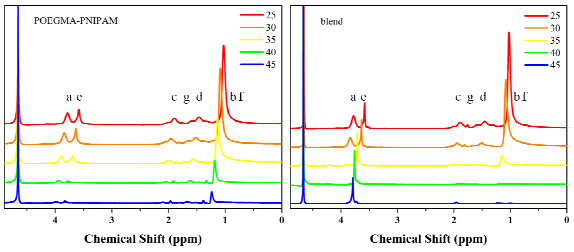

Fig. 2 Normalized temperature-variable ^{1}H NMR spectra of G25 and blend polymer with the same proportion in D_2O (10 wt %).

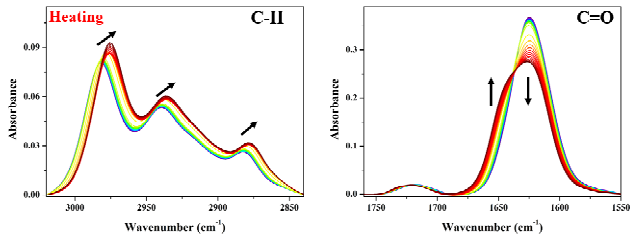

Fig. 3 Temperature-dependent FT-IR spectra of G25 in D_2O (10 wt %) during heating between 25 and 49°C with an interval of 1°C in the regions 3020-2840, 1760-1550 cm^{-1}.

Temperature-dependent FT-IR measurements of POEGMA-*g*-PNIPAM (G25) in D_2O (10 wt %) were performed during a heating process between 25 and 49 °C to elucidate the dynamic mechanism of the thermo-responsive behavior, as shown in Fig. 3. It should be noted that we used D_2O, rather than H_2O, as the solvent in order to eliminate the overlap of δ(O-H) band of H_2O around 1640 cm^{-1} with *ν*(C=O) of G25 as well as the broad *ν*(O-H) band of H_2O around 3300 cm^{-1} with *ν*(C-H) bands.[28] For the thermo-responsive PNIPAM segments, the transition temperature in D_2O is ca. 0.7 °C higher than that in H_2O.[29,30] Thus, the deuterium isotope effect can be considered to cause no obvious changes on the phase transition of G25.

Herein, we specifically focus on the following two spectral regions: C-H stretching region (3020-2840cm^{-1}) and C=O stretching region (1760-1550 cm^{-1}). In this way, we are able to trace almost all the group motions of G25 during the volume phase transition. As shown in Fig. 3, during the heating process, all the C-H stretching bands shift to lower frequency, indicating the changes of interactions between the hydrophobic moieties of the polymer and water molecules in the system. As is known, water clathrates exist around the hydrophobic moieties of water-soluble polymers in a well-ordered structure and more water molecules surrounding C-H groups would result in higher vibrational frequency.[31, 32] Thus it could be concluded that the C-H groups undergo dehydration with increasing temperature, which should mainly arise from the PNIPAM segments. As shown in Fig. 3, during heating, the amide I groups of PNIPAM show a binary spectral intensity change, similar to the spectral variation of pure PNIPAM in D_2O.[33] Generally, the *ν*(C=O) band can be roughly considered to be the combination of two bands at 1626 and 1651 cm^{-1}, which can be assigned to C=O stretching vibrations in C=O/D_2O and C=O/D–N hydrogen bonds, respectively. Thus the binary change of amide I in the PNIPAM segments during heating can be explained by the transformation of the hydrogen bonds of C=O from being with water to being self-associated ones.[32,34,35] Compared to amide I group of PNIPAM, the ester carbonyl group of POEGMA remains almost unchanged in the heating process. It is reasonable because POEGMA possesses no temperature-responsive property under this condition. Thus, generally speaking, together with the increase in hydrophobicity of the polymer chains, water molecules are expelled out of the polymer chains at the same time, as can be detected in the temperature-resolved FT-IR spectra.

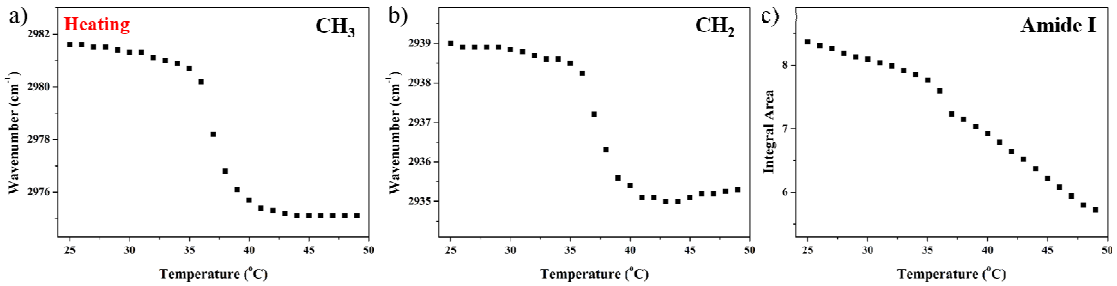

Fig. 4 Temperature-dependent frequency shifts of (a) ν_{as} (CH_3) and (b) ν_{as} (CH_2) as well as the integral area in the (c) Amide I region.

To quantitatively describe the phase transition processes during heating, the temperature-dependent frequency shifts of $\nu_{as}(CH_3)$ and $\nu_{as}(CH_2)$ as well as the half integral area of Amide I region have been plotted in Fig. 4. All the C-H stretching bands in 3020-2840 cm^{-1} shift to lower wavenumbers during heating due to the dehydration of polymer chains. Taking the middle point of the curve as the T_p, the T_p was determined to be around 36°C in both the $\nu_{as}(CH_3)$ and $\nu_{as}(CH_2)$ temperature-dependent frequency shift curves, which is in accordance with previous study. However, the integral area curve of the Amide I region is relatively unusual. Compared with the drastic change in PNIPAM system,[33] the change is relatively gentle and more conformational adjustment

are needed after the phase transition at around 36°C. The integral area of the eater group of POEGMA is not given as the change is too tiny to analyze. However, conventional 1DIR analysis cannot provide clear explanation for the phase transition behavior which will be further traced and clarified by following PCMW and 2Dcos analysis.

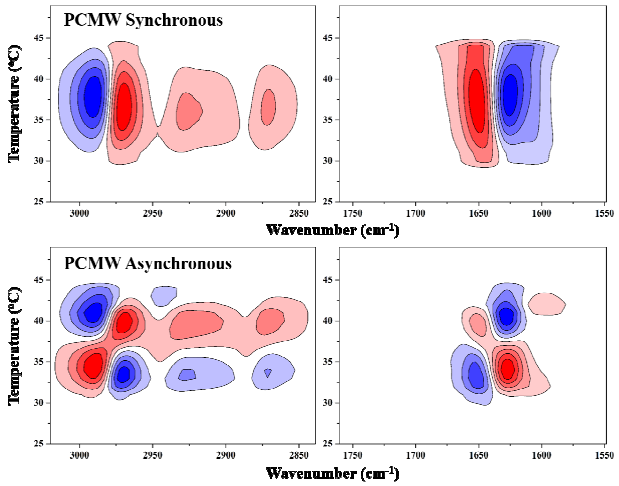

Fig. 5 PCMW synchronous and asynchronous spectra of G25 in D_2O (10 wt%) during heating between 25 and 49 °C. Warm colors (red) are defined as positive intensities, while cool colors (blue) as negative ones.

PCMW is a newly developed technique, whose basic principles can date back to conventional moving window proposed by Thomas et al.[36] Later in 2006 Morita et al. improved this technique to much wider applicability through introducing the perturbation variable into correlation equation.[37] PCMW is especially helpful to monitor spectral variations of different chemical systems, particularly weak phase transitions hard to observe by other methods. Except for its original ability in determining transition points as conventional moving window did, the technique additionally monitor complicated spectral variations along the perturbation direction. Fig. 5 presents PCMW synchronous and asynchronous spectra of G25 in D_2O during heating between 25 and 49 °C, respectively. For convenience, we plotted all the points read from PCMW synchronous and asynchronous spectra in Fig. 6. PCMW synchronous spectra are very helpful to find transition points. Thus, on average, for all the C–H and C=O bands, we have LCST to be ca. 36 °C during heating, in accordance with above results. However, different groups have apparently different responding temperatures. During heating C–H groups have earlier response than C=O groups. Additionally, it is worth noting that no peak of C=O group of POEGMA could be found in the synchronous and asynchronous spectra in PCMW, which means the phase transition degree is relative low. This could be attributed to the non-thermo-responsive property of POEGMA, which is also in good accordance with previous 1DIR study.

In addition to determining transition points, PCMW can also monitor the spectral variations along temperature perturbation combining the signs of synchronous and asynchronous spectra by the following rules: positive synchronous correlation represents spectral intensity increasing, while negative one represents decreasing; positive asynchronous correlation can be observed for a convex spectral intensity variation while negative one can be observed for a concave variation.[37] Based on this point, we can ascertain that during heating both the CH and C=O related bands of G25 show S-shaped or anti-S-shaped spectral changes, consistent with the above conventional IR analysis. The transition temperature region can also be determined by the peaks in the asynchronous spectra which are all turning points of the sigmoid curves. Then we can conclude that G25 experiences phase transition in D_2O mainly between 33 and 41 °C during heating. This served as an important basis for the segmental mode of the following 2Dcos analysis.

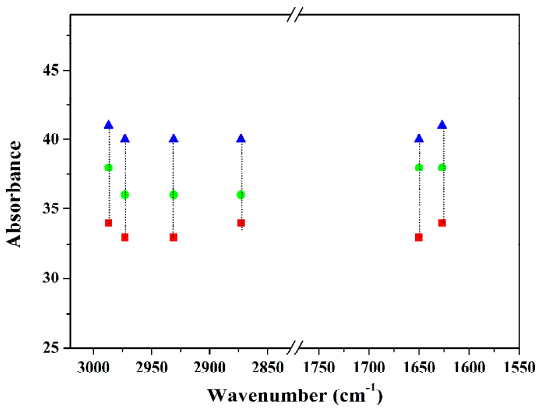

Fig. 6 Corresponding transition temperatures and transition temperature regions of G25 in D_2O (10 wt %) during heating read from PCMW synchronous and asynchronous spectra.

2Dcos is a mathematical method whose basic principles were first proposed by Noda in 1986.[38, 39] 2Dcos has been considerably applied to interpret spectroscopic intensity fluctuations under different types of external perturbations (e.g., temperature, pressure, concentration, time, electromagnetic) ever since.[40] By spreading the original spectra along a second dimension, features not readily visible in conventional analysis can be sorted out and hence, spectral resolution enhancement can be achieved. In addition, 2Dcos can be applied to deduce the specific sequence order of different chemical groups under a certain physical or chemical variable which cannot be obtained straight from conventional 1D spectra.

Table 2. Tentative Band Assignments of G25 According to 2Dcos Results.[28, 34, 35, 41] (The subscript $_N$ represents NIPAM while $_G$ represents OEGMA.)

Wavenumber(cm^{-1})	Assignment
2987	ν_{as}(hydrated CH_3)
2971	ν_{as}(dehydrated CH_3)
2942	ν_{as}(hydrated CH_2)
2931	ν_{as}(dehydrated CH_2)
2883	ν(CH)
2873	ν_s(CH_3)
1735	ν(C=O_G)
1700	ν(C=O_G…D_2O)
1646	ν(C=O_N…D-N_N)
1627	ν(C=O_N …D_2O)
1602	ν(C=O_N …2D_2O)

On the basis of the phase transition evolving regions obtained from PCMW, we chose all the spectra of G25 between 33 and 41 °C to perform 2Dcos analysis and the obtained synchronous and the asynchronous spectra are shown in Fig. 7.

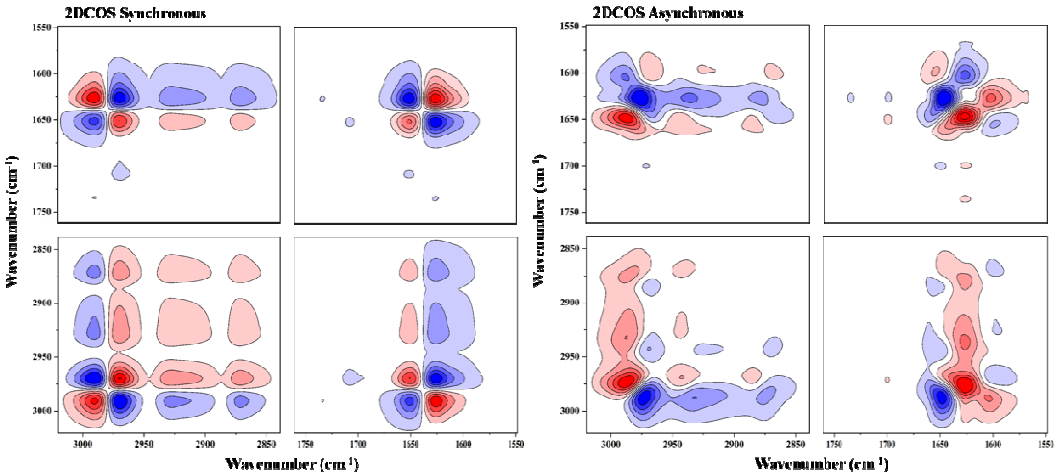

Fig. 7 2D synchronous and asynchronous spectra of G25 in D_2O (10 wt %) during heating. Warm colors (red) are defined as positive intensities, while cool colors (blue) as negative ones.

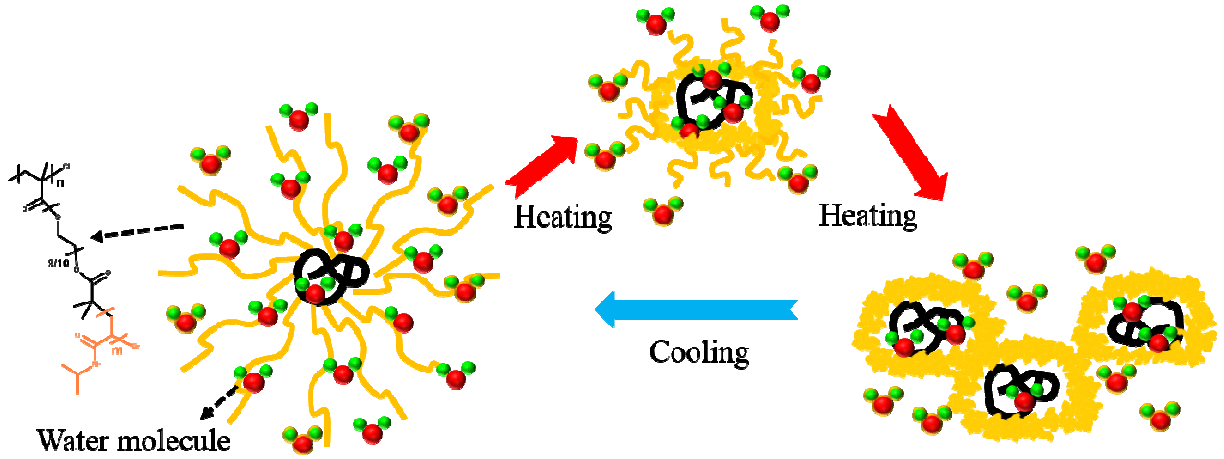

Scheme 2. Schematic illustration of the dynamic mechanism of the phase transition of POEGMA-*g*-PNIPAM in D_2O during the heating and cooling processes.

2D synchronous spectra provide information on simultaneous changes between two wavenumbers. For instance, the bands relating to C=O group of PNIPAM segments have negative cross-peaks, indicating that they display opposite sensitivities to temperature perturbation, that is, one decrease with the other increasing during heating determined from raw spectra. 2Dasynchronous spectra can significantly enhance the resolution of the original spectra. In Fig. 7, many subtle bands such as the bands at 2883 cm^{-1} and 1602 cm^{-1} attributed from ν_s(CH) and ν(C=O_N …2D_2O) that can't be determined in the 1D analysis have been identified. These additionally observed bands relating to subtle group conformations could provide more detailed information and significantly assist in figuring out the mechanism of the complex phase transition process. For clarity, all the bands found in asynchronous spectra and their corresponding assignments have been presented in Table 2.

In addition to enhancing spectral resolution, 2Dcos can also provide useful information on the specific sequence order of the chemical groups taking place under external perturbation. The judging rule can be summarized as Noda's role-that is, if cross-peaks (ν_1, ν_2, assume ν_1>ν_2) in the synchronous and asynchronous maps have the same symbol, both positive or both negative, then we can conclude that change at$\nu_1$occurs prior to that at ν_2 with the perturbation; whereas if cross-peaks (ν_1, ν_2) in the synchronous and asynchronous maps have different symbols, one positive and the other one negative, then we can infer that peak ν_2 varies prior to peak ν_1.[42]

The determination details of sequential orders have been presented in the Supporting Information, and here the final sequence order during heating is described as(→ means earlier than or prior to): 2942 cm^{-1}→ 1735 cm^{-1}→ 2883 cm^{-1}→1602 cm^{-1}→ 1646 cm^{-1}→2931 cm^{-1}→ 2971cm^{-1}→ 2873 cm^{-1}→ 1627 cm^{-1}→ 2987 cm^{-1} → 1700 cm^{-1}, or ν_{as}(hydrated CH_2) →ν(C=O_G) →ν(CH) →ν(C=O_N …2D_2O) → ν(C=O_N…D-N_N) →ν_{as}(dehydrated CH_2) → ν_{as}(dehydrated CH_3) → ν_s(CH_3)→ ν(C=O_N …D_2O)→ν_{as}(hydrated CH_3) →ν(C=O_G…D_2O).

Without considering the differences in stretching modes of the chemical groups, the specific order can be displayed as follows: CH_2 → C=O_G → CH → C=O_N → CH_3. However, as CH_2 and CH_3 exist in both NIPAM and OEGMA segments, it is hard to distinguish them with much detail. Another noticeable phenomenon is that both the 2D synchronous and asynchronous

spectra of POEGMA segments during heating are blank, only the cross peak between C=O group of POEGMA and PNIPAM could be detected, implying that the phase transition behavior of POEGMA was closely connected to PNIPAM. During the heating process, the $C{=}O_G$ groups response earlier than $C{=}O_N$, which implies that the driving force should be the dehydration of POEMGA-OH. However, as is known, POEGMA possesses no thermo-responsive property in this temperature region, and POEMGA-OH is located close to PNIPAM. Thus we can conclude the PNIPAM close to POEGMA would result in the dehydration of POEMGA. However, the PNIPAM close to or far from POEGMA might not be easy to be directly differentiated, the response order of POEGMA could provide indirect information. Combining our previous discussion, we can conclude that the inner zone of PNIPAM responses earlier than that located in the outer zone.

Based on the analysis above, herein, a two-step collapse mechanism was proposed as shown in Scheme 2. Double phase transition temperature was observed in the polymer brush due to the existence of POEGMA core which is favorable to the hydrophilic condition. PNIPAM in the inner zone was densely packed while less hydrated. However, restricted coil-like conformation were adopted in the outer zone. When the aqueous solutions of the copolymers were heated, the PNIPAM in the inner zone responses earlier with higher inter-chain cooperativity, which could account for the first transition. With further increasing temperature, PNIPAM in the outer zone collapsed gradually to form the densely packed shell within a relatively broad temperature range, and the second transition was observed. Notably, due to the restrictions on the collapse of the PNIPAM chain, the hydrophilic domains within the vitrified polymer may hinder the transport of water molecules from the inner zone to the outer zone although water might remain finely dispersed within the polymer matrix. Therefore, higher phase transition temperature compared with aqueous dispersions of PNIPAM brushes covalently bound to the surface of gold nanoparticles and hydrophobic hyperbranched polyester core was observed.

Conclusions

In summary, PNIPAM brush integrating hydrophilic POEGMA core was synthesized *via* successive ATRP process with *grafting from* methods. Due to the decoupling effect of long flexible ethylene glycol spacers and the large molar ratio between PNIPAM and POEGMA, core-shell morphology with coiled POEMGA main chains was observed in the copolymers. Compared with aqueous dispersions of PNIPAM brushes covalently bound to the surface of gold nanoparticles and hydrophobic hyperbranched polyester core, increment of the double phase transition temperature was observed due to the existence of POEGMA core which was favourable to the hydrophilic condition. Thermally induced phase transition behavior of NIPAM brushes was investigated with ^{1}H NMR and FT-IR spectroscopy in combination with PCMW and 2Dcos analysis at the molecular level. Phase transition temperature (ca. 36 °C) during heating as well as transition temperature range (33–41 °C) was determined by PCMW analysis. 2Dcos was employed to discern the sequence order of group motions during heating and it is concluded that the PNIPAM in the inner zone responses earlier than that located in the outer zone.

Acknowledgements

We are very grateful for the financial support of the National Natural Science Foundation of China (NSFC) (No. 21274030).

Notes and references

† Electronic Supplementary Information (ESI) available: [Detailed synthesis procedure and characterization information are available].

State Key Laboratory of Molecular Engineering of Polymers, Ministry of Education, Department of Macromolecular Science, and Laboratory of Advanced Materials, Fudan University, Shanghai 200433, China. E-mail: peiyiwu@fudan.edu.cn (Peiyi Wu)

1. B. Yameen and A. Farrukh, *Chem.-Asian J.*, 2013, **8**, 1736-1753.
2. A. Rastogi, M. Y. Paik, M. Tanaka and C. K. Ober, *ACS Nano*, 2010, **4**, 771-780.
3. R. Barbey and H. A. Klok, *Langmuir*, 2010, **26**, 18219-18230.
4. H. I. Lee, J. Pietrasik, S. S. Sheiko and K. Matyjaszewski, *Prog. Polym. Sci.*, 2010, **35**, 24-44.
5. W. J. Brittain, S. G. Boyes, A. M. Granville, M. Baum, B. K. Mirous, B. Akgun, B. Zhao, C. Blickle and M. D. Foster, in *Surface- Initiated Polymerization Ii*, ed. R. Jordan, Springer-Verlag Berlin, Berlin, 2006, vol. 198, pp. 125-147.
6. H. Wei, S. X. Cheng, X. Z. Zhang and R. X. Zhuo, *Prog. Polym. Sci.*, 2009, **34**, 893-910.
7. Y. Ono and T. Shikata, *J. Am. Chem. Soc.*, 2006, **128**, 10030-10031.
8. K. J. Zhou, Y. J. Lu, J. F. Li, L. Shen, G. Z. Zhang, Z. W. Xie and C. Wu, *Macromolecules*, 2008, **41**, 8927-8931.
9. P. W. Zhu and D. H. Napper, *J. Colloid Interface Sci.*, 1994, **164**, 489-494.
10. J. Shan, J. Chen, M. Nuopponen and H. Tenhu, *Langmuir*, 2004, **20**, 4671-4676.
11. J. Shan, Y. M. Zhao, N. Granqvist and H. Tenhu, *Macromolecules*, 2009, **42**, 2696-2701.
12. J. Zhao, J. Shan, G. Van Assche, H. Tenhu and B. Van Mele, *Macromolecules*, 2009, **42**, 5317-5327.
13. J. Xu, S. Z. Luo, W. F. Shi and S. Y. Liu, *Langmuir*, 2006, **22**, 989-997.
14. S. Z. Luo, J. Xu, Z. Y. Zhu, C. Wu and S. Y. Liu, *J. Phys. Chem. B*, 2006, **110**, 9132-9139.
15. M. Wagner, F. Brochardwyart, H. Hervet and P. G. Degennes, *Colloid Polym. Sci.*, 1993, **271**, 621-628.
16. P. G. Degennes, *Comptes Rendus De L Academie Des Sciences Serie Ii*, 1991, **313**, 1117-1122.
17. H. G. Schild, *Prog. Polym. Sci.* **1992**, *17*, 163-249.
18. S. Z. Luo, J. Xu, Z. Y. Zhu, C. Wu, S. Y. Liu, *J. Phys. Chem. B* **2006**, *110*, 9132-9138.
19. C. M. Li, N. Gunari, K. Fischer, A. Janshoff and M. Schmidt, *Angew. Chem. Int. Ed.*, 2004, **43**, 1101-1104.
20. S. S. Sheiko, B. S. Sumerlin and K. Matyjaszewski, *Prog. Polym. Sci.*, 2008, **33**, 759-785.
21. S. Z. Luo, X. L. Hu, Y. Y. Zhang, C. X. Ling, X. Liu and S. S. Chen, *Polymer Journal*, **43**, 41-50.

22. C. Li, Z. Ge, H. Liu, S. Liu, *J. Polym. Sci. Part A* **2009**, 47, 4001-4013.
23. C. M. Burba, S. M. Carter, K. J. Meyer and C. V. Rice, *J. Phys. Chem. B*, 2008, **112**, 10399-10404.
24. G. Y. Ru, N. Wang, S. H. Huang and J. W. Feng, *Macromolecules*, 2009, **42**, 2074-2078.
25. O. C. Compton, S. W. Cranford, K. W. Putz, Z. An, L. C. Brinson, M. J. Buehler and S. T. Nguyen, *ACS Nano*, 2012, **6**, 2008-2019.
26. C. L. Bao, Y. Q. Guo, L. Song and Y. Hu, *J. Mater. Chem.*, 2011, **21**, 13942-13950.
27. K. Van Durme, G. Van Assche, V. Aseyev, J. Raula, H. Tenhu and B. Van Mele, *Macromolecules*, 2007, **40**, 3765-3772.
28. S. T. Sun and P. Y. Wu, *Macromolecules*, 2013, **46**, 236-246.
29. H. Shirota, N. Kuwabara, K. Ohkawa and K. Horie, *J. Phys. Chem. B*, 1999, **103**, 10400-10408.
30. X. H. Wang and C. Wu, *Macromolecules*, 1999, **32**, 4299-4301.
31. E. C. Cho, J. Lee and K. Cho, *Macromolecules*, 2003, **36**, 9929-9934.
32. P. Schmidt, J. Dybal and M. Trchova, *Vib. Spectrosc.*, 2006, **42**, 278-283.
33. B. J. Sun, Y. N. Lin, P. Y. Wu and H. W. Siesler, *Macromolecules*, 2008, **41**, 1512-1520.
34. S. T. Sun, W. D. Zhang, W. Zhang, P. Y. Wu and X. L. Zhu, *Soft Matter*, 2012, **8**, 3980-3987.
35. S. T. Sun, J. Hu, H. Tang and P. Y. Wu, *Phys. Chem. Chem. Phys.*, 2011, **13**, 5061-5067.
36. M. Thomas and H. H. Richardson, *Vib. Spectrosc.*, 2000, **24**, 137-146.
37. S. Morita, H. Shinzawa, I. Noda and Y. Ozaki, *Appl. Spectrosc.*, 2006, **60**, 398-406.
38. I. Noda, *Appl. Spectrosc.*, 1993, **47**, 1329-1336.
39. I. Noda, A. E. Dowrey, C. Marcott, G. M. Story and Y. Ozaki, *Appl. Spectrosc.*, 2000, **54**, 236A-248A.
40. I. Noda, *J. Mol. Struct.*, 2008, **883**, 2-26.
41. S. T. Sun, J. Hu, H. Tang and P. Y. Wu, *J. Phys. Chem. B*, 2010, **114**, 9761-9770.
42. I. Noda, *Appl. Spectrosc.*, 2000, **54**, 994-999.

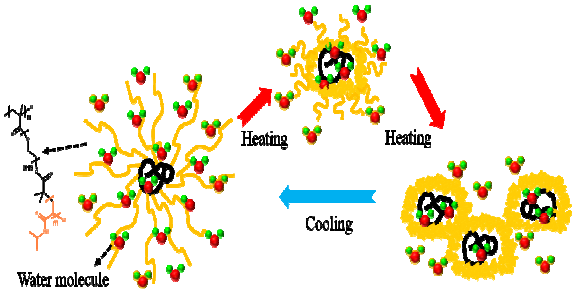

dynamic mechanism of the phase transition of POEGMA-*g*-PNIPAM in D_2O during the heating and cooling processes.